ACADÉMIE
DES SCIENCES
INSTITUT DE FRANCE

Comptes Rendus
Mécanique

Luoyu Roy Xu and Yuelong Jiang

A simple model for estimating the crack kinking angles of pure shear fracture of 3D printing polymers

Volume 354 (2026), p. 25-33

Online since: 16 January 2026

https://doi.org/10.5802/crmeca.311

The Comptes Rendus. Mécanique *are a member of the Mersenne Center for open scientific publishing*
www.centre-mersenne.org — e-ISSN : 1873-7234

ACADÉMIE DES SCIENCES
INSTITUT DE FRANCE

Comptes Rendus. Mécanique
2026, Vol. 354, p. 25-33
https://doi.org/10.5802/crmeca.311

Research article

A simple model for estimating the crack kinking angles of pure shear fracture of 3D printing polymers

Luoyu Roy Xu [*,a] **and Yuelong Jiang** [a]

[a] School of Mechanical Engineering and Mechanics, Ningbo University, Zhejiang, China

E-mail: l.roy.xu@alumni.caltech.edu (L. R. Xu)

Abstract. Shear fracture studies of three-dimensional (3D) printing polymers with interfaces were rarely reported due to their complicated mechanics and material issues. In this study, a short-beam shear fracture approach was employed to characterize the mode-II shear fracture toughness of polyamide specimens of three printing surface angles made with selective laser sintering (SLS). Results show that a pure shear crack only existed if the initial crack propagated along the printing interface. In other cases, initial cracks kinked right after crack initiation, so no valid shear fracture toughness was measured. A simple model based on linear elastic fracture mechanics including anisotropic fracture toughnesses was proposed to predict the crack kinking angles. The prediction agreed with the measurements well and was more reasonable than the prediction based on the maximum tensile stress criterion.

Keywords. Shear fracture, Fracture toughness, 3D printing, Polymer, Interfaces.

Note. Article submitted by invitation.

Manuscript received 24 January 2025, revised and accepted 18 June 2025, online since 16 January 2026.

1. Introduction

The mode-II fracture toughness has long been a difficult property to quantify for isotropic materials, because a mode-II crack tends to kink away from the original crack path [1], and thereby makes the measured fracture toughness the mode-I fracture toughness. However, a pure mode-II crack may exist in some special materials with preferred interfaces like layered materials, or composite materials [2]. Indeed, layered 3D printing materials have numerous interfaces between the printing layers as the weak paths for potential crack propagation. With the growing applications of 3D printing materials, it is important to develop new approaches to measure their mode-II shear fracture toughnesses because of their anisotropic strengths and fracture toughnesses [3,4]. 3D printing materials based on single-material printing can be treated as isotropic and homogenous materials in terms of stiffness because no second material (only defects such as voids) exists in the printed materials. However, their strengths and fracture toughnesses were slightly anisotropic due to the printing interfaces and the intrinsic build direction that led to initial defects in different directions [5–7]. It should be noted that their anisotropic degree was much lower than the layered composite materials [8].

* Corresponding author

There were a few shear fracture experiments of 3D printing polymers in the open literature. But two major issues were found, (1) a pure shear stress field ahead of a shear crack was not shown, and (2) the initial shear crack might kink right away. For example, Khan et al. [9] employed 3D printing polymer specimens for the mode-I, II and mixed-mode fracture toughness tests, but the above critical fracture mechanics issues were not addressed. Therefore, whether their measured values can be treated as valid fracture toughnesses or not is still a big question. Hence, to measure the valid mode-II fracture toughnesses of 3D printing polymers, a short-beam shear fracture (SBSF) approach initially proposed by Krishnan and Xu [10] was modified to eliminate the friction between the cracked surfaces, and ensure a pure shear stress field, thereby offering a more reasonable value of the mode-II fracture toughness. Another advantage of the SBSF approach was that the shear crack propagated along the initial crack path if the initial crack path was along the interface, not immediately kinked from the initial crack. If the initial crack path was not along the interface, the initial crack might kink right after the crack initiation. Crack kinking is a special fracture problem, and it has been received long-term attention since it can occur during static and dynamic loading processes [11–14]. Hence, in this paper, a simple model using linear elastic fracture mechanics (LEFM) was employed to analyze the crack kinking during a pure shear fracture experiment. The purpose of this study was to predict the crack kinking angles if the initial crack kinked.

2. Theory

2.1. *Stress intensity factors of a kinked crack including the T-stress*

As shown in Figure 1, based on LEFM, the two-dimensional full-field stress of a main crack can be expressed in a polar coordinate system [15]:

$$\sigma_{ij}(r,\theta) = \frac{K_{\mathrm{I}}}{\sqrt{2\pi r}} \sum_{ij}^{\mathrm{I}}(\theta) + T\delta_{i1}\delta_{j1} + \frac{K_{\mathrm{II}}}{\sqrt{2\pi r}} \sum_{ij}^{\mathrm{II}}(\theta) + O(r^{\frac{1}{2}}) \qquad (i,j=1,2) \tag{1}$$

where K_{I} and K_{II} are the mode-I and mode-II stress intensity factors, T is a nonsingular stress term, $O(r^{\frac{1}{2}})$ represents the higher-order terms of the length scale r and will be dropped if the kinked crack length "l" is very small; and the known functions $\Sigma_{ij}^{\mathrm{I}}(\theta), \Sigma_{ij}^{\mathrm{II}}(\theta)$ represent the angular variations of the 2-D stress components. Previous research on crack kinking was mainly focused on the relation between the stress intensity factors before and after crack kinking [16]. If the T-stress is considered during crack kinking, the two stress intensity factors of the kinked crack k_{I} and k_{II} became [11,17]:

$$k_1 = C_{11}K_{\mathrm{I}} + C_{12}K_{\mathrm{II}} + 2T\sqrt{\frac{2l}{\pi}}\sin^2\beta \tag{2}$$

$$k_2 = C_{21}K_{\mathrm{I}} + C_{22}K_{\mathrm{II}} - 2T\sqrt{\frac{2l}{\pi}}\sin\beta\cos\beta \tag{3}$$

where β is the kinking angle, i.e., the angle between the main crack and the kinked crack as seen in Figure 2. The coefficients C_{ij} $(i,j=1,2)$ were initially reported by Contrell and Rice [16]:

$$C_{11} = \left(\frac{3}{4}\cos\frac{\beta}{2} + \frac{1}{4}\cos\frac{3\beta}{2}\right) \qquad C_{12} = -\frac{3}{4}\left(\sin\frac{\beta}{2} + \sin\frac{3\beta}{2}\right) \tag{4}$$

$$C_{21} = \left(\frac{1}{4}\sin\frac{\beta}{2} + \frac{1}{4}\sin\frac{3\beta}{2}\right) \qquad C_{22} = \left(\frac{1}{4}\cos\frac{\beta}{2} + \frac{3}{4}\cos\frac{3\beta}{2}\right). \tag{5}$$

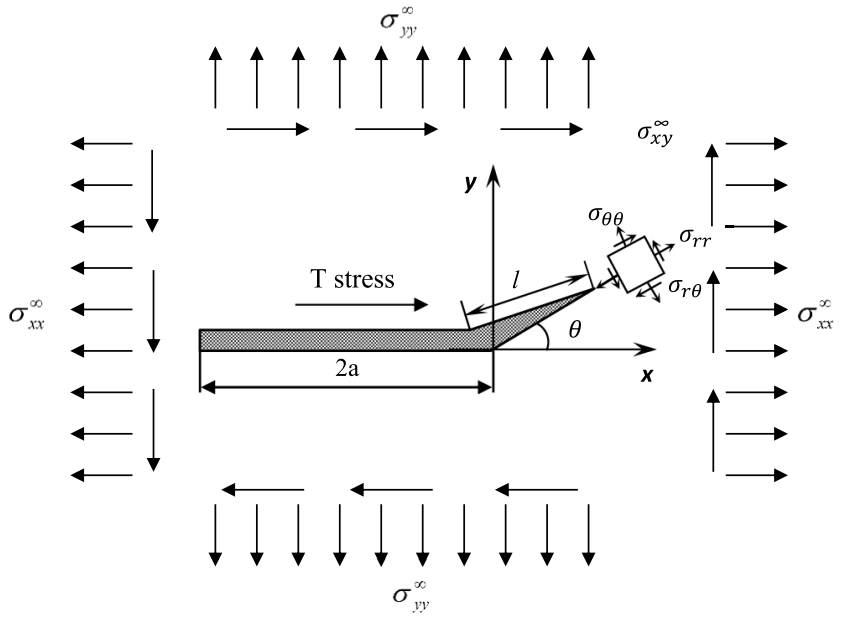

Figure 1. Schematic of a kinked crack (with a very small length l) initiating from a main crack (length 2a) subjected to remote 2-D mixed-mode loading. The local stress field at the kinked crack tip is shown in a polar coordinate system.

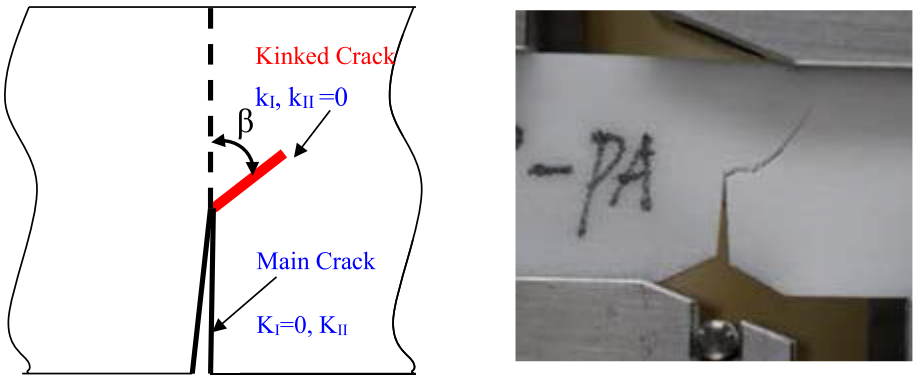

Figure 2. Schematic diagram of a kinked crack (left), and a photo of the actual crack kinking of a shear fracture 3D printed specimen under loading (right).

Now we consider a shear main crack with $K_{\mathrm{I}} = 0$, and assume the kinked crack is a mode-I crack ($k_2 = 0$), Equations (2) and (3) yield:

$$k_1 = C_{12} K_{\mathrm{II}} + 2T\sqrt{\frac{2l}{\pi}}\sin^2\beta \tag{6}$$

$$k_2 = C_{22} K_{\mathrm{II}} - 2T\sqrt{\frac{2l}{\pi}}\sin\beta\cos\beta = 0. \tag{7}$$

Substitute Equation (7) into (6) to eliminate T and l, the mode-I stress intensity factor of the kinked crack becomes,

$$k_1 = (C_{12} + C_{22}\tan\beta)K_{\mathrm{II}}. \tag{8}$$

The kinked crack is often a mode-I crack because this conclusion was verified by the authors' dynamic fracture experiments using high-speed photography [14,18]. If $T = 0$,

$$k_2 = C_{22}(\beta)K_{\mathrm{II}} = 0, \quad \text{then } \beta \approx 70.5°. \tag{9}$$

Erdogan and Sih [19] proposed the maximum tensile stress (MTS) criterion (no T-stress was involved) and assumed that the kinked mode-I crack initiated in the direction corresponding to where the circumferential tensile stress around the crack tip reaches its maximum value. For a pure shear crack, the crack kinking angle predicted by the MTS criterion is around 70.5°, i.e., the same outcome.

2.2. *Energy-based fracture criterion for crack kinking from the interface*

As shown in Figure 3, a modified short-beam shear fracture specimen was proposed, and it was subjected to an asymmetric four-point bending load. Indeed, this was not a typical asymmetric four-point bending test because this experiment was conducted using an Iosipescu shear fixture as seen in Figure 4. The load acting on the specimen was distributed load, not point load as shown in Figure 3 for illustration purposes. The printing surface (interface) angles were 0°, 45°, and 90°. If the printing surface angle is 90°, the printed initial crack is along the interface (a weak path). For a mode-II main crack of an interfacial shear fracture toughness measurement, $K_{\mathrm{I}} = 0$. Therefore, a valid shear fracture experiment requires that continuous crack propagation along the original crack path occurs when the mode-II energy release rate, G_{II} exceeds the fracture toughness of the printing interface $\Gamma^{IT}_{\mathrm{II}C}$, i.e.,

$$G_{\mathrm{II}} = \frac{K^2_{\mathrm{II}}}{E^*} \geq \Gamma^{IT}_{\mathrm{II}C} \tag{10}$$

where $E^* = E$ for plane stress and $E^* = E/(1-\nu^2)$ for plane strain, and E is the Young's modulus of the material and ν is the Poisson's ratio. On the other hand, the initial crack will kink if the mode-I energy release rate of the kinked crack tip, g_{I}, exceeds the mode-I fracture toughness of the bulk printing material next to the printing interface, $\Gamma^{\mathrm{BM}}_{\mathrm{I}C}$, i.e.,

$$g_{\mathrm{I}} = \frac{k^2_{\mathrm{I}}}{E^*} \geq \Gamma^{\mathrm{BM}}_{\mathrm{I}C}. \tag{11}$$

Hence, crack kinking is only possible if this inequality holds:

$$\frac{g_{\mathrm{I}}}{G_{\mathrm{II}}} = [C_{12} + C_{22}\tan\beta]^2 > \frac{\Gamma^{\mathrm{BM}}_{\mathrm{I}C}}{\Gamma^{IT}_{\mathrm{II}C}} = \left(\frac{k^{\mathrm{BM}}_{\mathrm{I}C}}{K^{IT}_{\mathrm{II}C}}\right)^2 = \lambda. \tag{12}$$

Therefore, only the ratio of two independent fracture toughnesses λ determines the crack kinking angle. Indeed, the outcome of this paper will be applicable to more material systems with weak interfaces rather than 3D printing materials only.

3. Methods and materials

As shown in Figure 2, the printed notch had a variable width to conveniently cut a sharp notch using a fresh razor blade. At the bottom of the specimen, the notch had a sudden wide opening to avoid specimen/loading block contact when the applied load/displacement was large for the soft polymer specimens. For each printing surface angle, at least eight identical specimens were made and tested. It should be noted that for the 90° specimen, the printing surface/interface was along

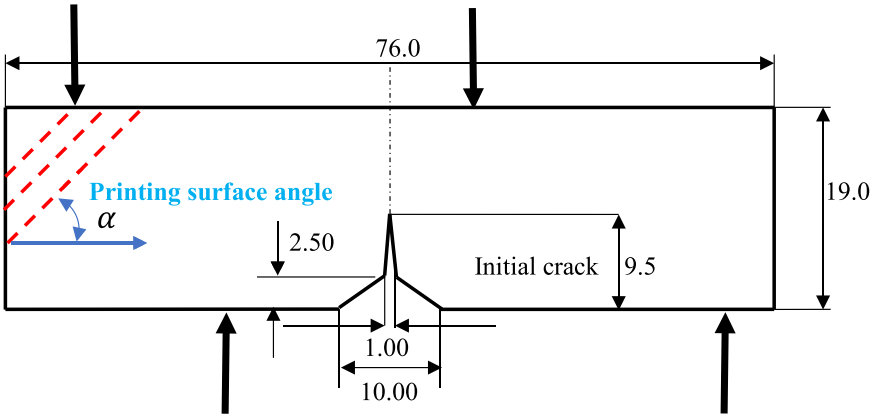

Figure 3. Size and applied load of a short-beam shear fracture specimen (All dimensions are in mm. The thickness was 4 mm). The printing surface angles α were 0°, 45°, and 90°.

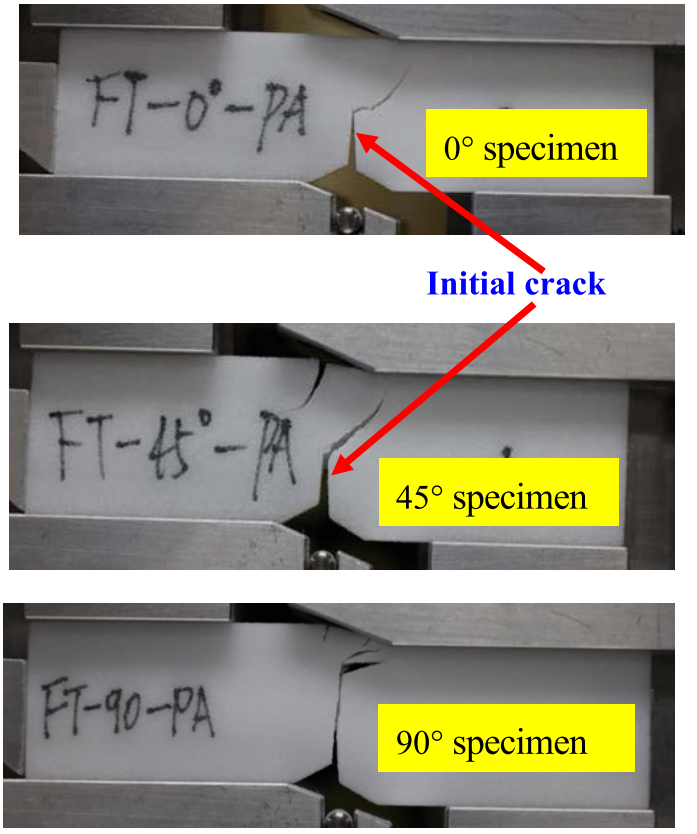

Figure 4. Failure modes of PA specimens with different printing surface angles.

the initial crack direction to measure the mode-II interlayer shear fracture toughness. To create polyamide (PA) specimens, PA powder (FS3300PA) with a spherical shape and a mean particle size of 120 μm was used, and the apparent density was 0.48 g/cm^3. A selective laser sintering apparatus (HT252P) was employed to make these specimens. The apparatus was equipped with

a 60 W carbon dioxide laser with a focal laser beam diameter of ≤0.5 mm. The processing parameters were set as follows: a laser power of 45 W, a laser scanning speed of 10 m/s, and a layer thickness of 0.1 mm. A heater was equipped to preheat the raw powder material, capable of reaching a maximum temperature of up to 225 °C. During the printing process, the chamber was filled with high-purity nitrogen to protect the specimens from oxidation. All fracture specimens were tested on an Instron 5966 test frame equipped with a 10 kN load cell using an Iosipescu shear fixture. The displacement rate for all tests was set at 1 mm/min, and the maximum loadings of the specimens were recorded. Photos were taken from some specimens to record the final crack pattern before they were removed from the test machine. More experimental details will be reported by Wang et al. [20].

4. Results and discussion

4.1. *Crack kinking in different specimens with different printing surface angles*

Figure 4 shows two different fracture modes of three types of shear fracture specimens. For the specimens with the printing surface angles of 0° and 45°, the crack kinked from the initial crack right after its initiation and formed a mode-I crack as seen in almost all homogenous materials subjected to a pure shear load. For the specimens with the printing surface angle of 90°, the initial shear crack propagated along the initial crack path. Based on the energy release rate definition, a crack creates the fracture surface in an in-plane shear pattern after crack initiation. Hence, it is concluded that the mode-II shear fracture toughness for the 90° specimens is valid. It is important to note that this crack finally kinked but it was caused by the mixed load (not pure shear load) because of the large specimen deformation and the close distance of the crack tip and the load block. The propagation of an interfacial crack is a more complicated case [11,21], therefore, it is not considered in this simple study. However, for the 0° and 45° specimens, the crack created the fracture surface in an opening mode, so a valid shear fracture toughness was not obtained for these two specimens.

Therefore, the measured shear fracture toughness of 90° specimens was the interlayer shear fracture toughness because a shear crack only existed in the weak printing interfaces between different layers. The measured mode-II fracture toughness based on LEFM of the printing interface $K_{\mathrm{IIC}}^{\mathrm{I}T}$ (2.57 MPa·m$^{1/2}$) was slightly more than the mode-I fracture toughness of the printing interface $K_{\mathrm{I}C}^{\mathrm{I}T}$ (2.30 MPa·m$^{1/2}$) for the same material interface/same specimen thickness [22]. The $K_{\mathrm{II}C}$ of the printing interface was obtained as

$$K_{\mathrm{IIC}}^{\mathrm{I}T} = \frac{P_{\mathrm{C}}}{Wt}\sqrt{\pi a}F_{\mathrm{II}}^{\mathrm{SBSF}}\left(\frac{a}{W}\right) \tag{13}$$

where $F_{\mathrm{II}}^{\mathrm{SBSF}}$ is a dimensionless parameter [10], and P_{C} is the critical load at crack initiation, W is the specimen width, t is the specimen thickness, and a is the crack length. This fracture toughness indicated that there was little friction between the cracked faces, because friction led to significant energy dissipation and inaccurately contributed to the fracture toughness.

4.2. *Crack kinking analysis based on the proposed model*

The measured crack kinking angles are listed in Table 1. The predicted kinking angle according to the MTS criterion was 70°, i.e., between the kinking angles of the 0° specimen and the 45° specimen. This inaccuracy is probably caused by the two disadvantages of the MTS criterion: (1) the crack kinking angle is independent of the material properties (e.g., fracture toughness), and (2) the T-stress is neglected.

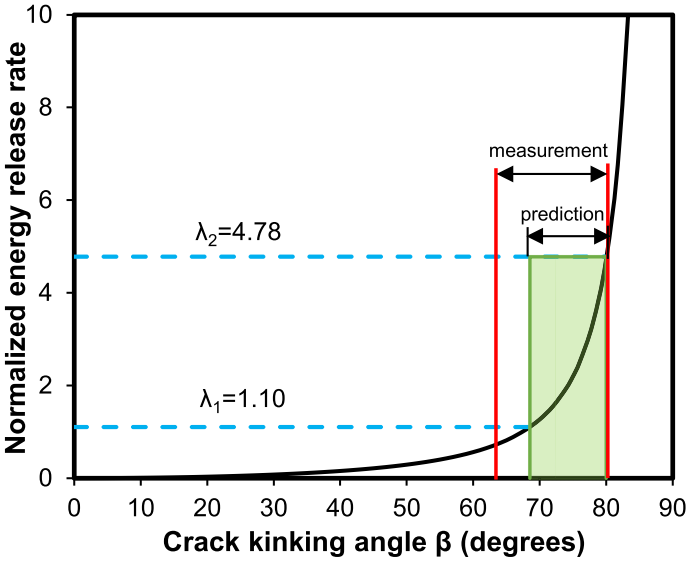

Figure 5. Normalized energy release rate g_I/G_{II} as a function of the crack kinking angle. The predicted crack kinking angles were 68° to 80°, while the actual crack kinking angles were 64° to 80°.

Table 1. Crack kinking angles of the specimen with different printing surface angles

	0° specimens	45° specimens
Crack kinking angle Ω	79.92 ± 7.07	64.13 ± 12.31

The proposed model does not have these disadvantages and clearly shows the dependence of the crack kinking angles on the fracture toughness as seen in the Equation (12). About the potential range of the ratio of two independent fracture toughnesses λ, it is difficult to measure the fracture toughness of the printing layer. However, the mode-I intralayer fracture toughness of the 3D printing layer is always lower than the mode-I fracture toughness of the traditional polymers (e.g., inject-molding) due to fewer initial defects. Therefore, the mode-I intralayer fracture toughness of the bulk PA is around 2.70 to 5.62 MPa·m$^{1/2}$ based on previous measurements [23], or $\lambda_1 = 1.10$ and $\lambda_2 = 4.78$. Their corresponding crack kinking angles are 68° to 80°, while the actual crack kinking angles are 64° to 80° as shown in Figure 5. Obviously, our prediction is better than the MTS criterion.

However, our simple model cannot predict the different crack kinking angles for the 0° and the 45° specimens individually, although they are indeed different as shown in Table 1. Because our model assumes that the interface/printing surface has no thickness like numerous traditional interface mechanics models. If we assume that the interface/printing surface has a thickness, its thickness becomes a variable for different materials and might become a fitting parameter rather than a material constant. However, for a specific 3D printing technique, the interface thickness should be treated as a material constant, and it should be less than 1% of the thickness of a printing layer although there are no direct measurements. For example, for the current PA specimen made with SLS, its layer thickness is 0.1 mm, so the thickness of the printing interface should be below 100 μm. Also, the PA powder had a mean diameter of 120 μm before the SLS process, therefore, an upper limit of 100 μm is a reasonable assumption for the thickness of the SLS printing interfaces. Anyway, the anisotropic feature of the interfaces should be considered

for future sophisticated models. Also, the material properties of the finite interfaces could be assumed to be different from the properties of the printing layers.

5. Conclusions

A simple model based on linear elastic fracture mechanics including anisotropic fracture toughnesses was proposed to predict the crack kinking angles. The prediction agreed with the measurements well and was more reasonable than the prediction based on the maximum tensile stress criterion. Future new models should consider the anisotropic features/thickness of the interfaces in order to predict the crack kinking more reasonably.

Declaration of interests

The authors do not work for, advise, own shares in, or receive funds from any organization that could benefit from this article, and have declared no affiliations other than their research organizations.

References

[1] T. L. Anderson, *Fracture Mechanics: Fundamentals and Applications*, 3rd edition, CRC Press: Boca Raton, 2004.
[2] D. Coker and A. J. Rosakis, "Experimental observations of intersonic crack growth in asymmetrically loaded unidirectional composite plates", *Philos. Mag. A* **81** (2001), pp. 571–595.
[3] T. Brugo, R. Palazzetti, S. Ciric-Kostic, X. T. Yan, G. Minak and A. Zucchelli, "Fracture mechanics of laser sintered cracked polyamide for a new method to induce cracks by additive manufacturing", *Polym. Test.* **50** (2016), pp. 301–308.
[4] E. Monaldo, M. Ricci and S. Marfia, "Mechanical properties of 3D printed polylactic acid elements: experimental and numerical insights", *Mech. Mater.* **177** (2023), article no. 104551.
[5] L. R. Xu and D. Leguillon, "Dual-notch defect model to understand the anisotropic strengths of 3d printed polymers", *ASME J. Eng. Mater. Technol.* **142** (2020), no. 2020, article no. 14501.
[6] Q. Wang, G. Zhang, X. Zheng, Y. Ni, F. Liu, Y. Liu and L. R. Xu, "Efficient characterization on the interlayer shear strengths of 3D printing polymers", *J. Mater. Res. Technol.* **22** (2023), pp. 2768–2780.
[7] G. Zhang, Q. Wang, Y. Ni, P. Liu, F. Liu, D. Leguillon and L. R. Xu, "A systematic investigation on the minimum tensile strengths and size effects of 3D printing polymers", *Polym. Test.* **117** (2023), article no. 107845.
[8] I. M. Daniel and O. Ishai, *Engineering Mechanics of Composite Materials*, Oxford University Press: New York, 2005.
[9] A. S. Khan, A. Ali, G. Hussain and M. Ilyas, "An experimental study on interfacial fracture toughness of 3-D printed ABS/CF-PLA composite under mode I, II, and mixed-mode loading", *J. Thermoplast. Compos. Mater.* **34** (2019), pp. 1599–1622.
[10] A. Krishnan and L. R. Xu, "A short-beam shear fracture approach to measure the mode II fracture toughness of materials with preferred interfaces", *Int. J. Fract.* **169** (2011), pp. 15–25.
[11] J. W. Hutchinson and Z. Suo, "Mixed mode cracking in layered materials", *Adv. Appl. Mech.* **29** (1992), pp. 63–191.
[12] J.-B. Leblond and J. Frelat, "Crack kinking from an initially closed crack", *Int. J. Solids Struct.* **37** (2000), no. 11, pp. 1595–1614.
[13] J.-B. Leblond and J. Frelat, "Crack kinking from an interface crack with initial contact between the crack lips", *Eur. J. Mech.—A/Solids* **20** (2001), no. 6, pp. 937–951.
[14] L. R. Xu, Y. Y. Huang and A. J. Rosakis, "Dynamic crack deflection and penetration at interfaces in homogeneous materials: experimental studies and model predictions", *J. Mech. Phys. Solids* **51** (2003), pp. 461–486.
[15] A. T. Zehnder, *Fracture Mechanics*, Springer: New York, 2012.
[16] B. Cotterell and J. R. Rice, "Slightly curved or kinked cracks", *Int. J. Fract.* **16** (1980), no. 1980, pp. 155–169.
[17] X.-F. Li and L. R. Xu, "T-stresses across static crack kinking", *J. Appl. Mech.* **74** (2007), pp. 181–190.
[18] L. R. Xu and A. J. Rosakis, "An experimental study on dynamic failure events in homogeneous layered materials using dynamic photoelasticity and high-speed photography", *Opt. Laser Eng.* **40** (2002), no. 2003, pp. 263–288.
[19] F. Erdogan and G. C. Sih, "On the crack extension in plates under plane loading and transverse shear", *J. Basic Eng.* **85** (1963), pp. 519–525.
[20] Q. Wang, G. Zhang, X. Zheng and L. R. Xu, "Experimental study on the shear fracture toughness of 3D printing polyamide", 2025. under review.

[21] V.-X. Tran, D. Leguillon, A. Krishnan and L. R. Xu, “Interface crack initiation at V-notches along adhesive bonding in weakly bonded polymers subjected to mixed-mode loading”, *Int. J. Fract.* **176** (2012), pp. 65–79.

[22] G. Zhang, J. Ghorbani, X. Zheng, et al., “Anisotropic and elastoplastic mode-I fracture toughnesses of three additively manufactured polymers fabricated via material extrusion and powder bed fusion”, *Fatigue Fract. Eng. Mater. Struct.* **46** (2023), pp. 4776–4782.

[23] *Materials Databook*, University of Cambridge Engineering Department, 2003.